Cell Reports

Pax3 and Hippo Signaling Coordinate Melanocyte Gene Expression in Neural Crest

Graphical Abstract

Highlights

Taz and Yap65 are Pax coactivator molecules and function at Pax targets

Pax3-Taz/Yap65 activity requires Pax3-DNA binding but is Tead independent

Hippo kinases Mst1 and Lats2 can inhibit the Pax3-Taz/Yap complex
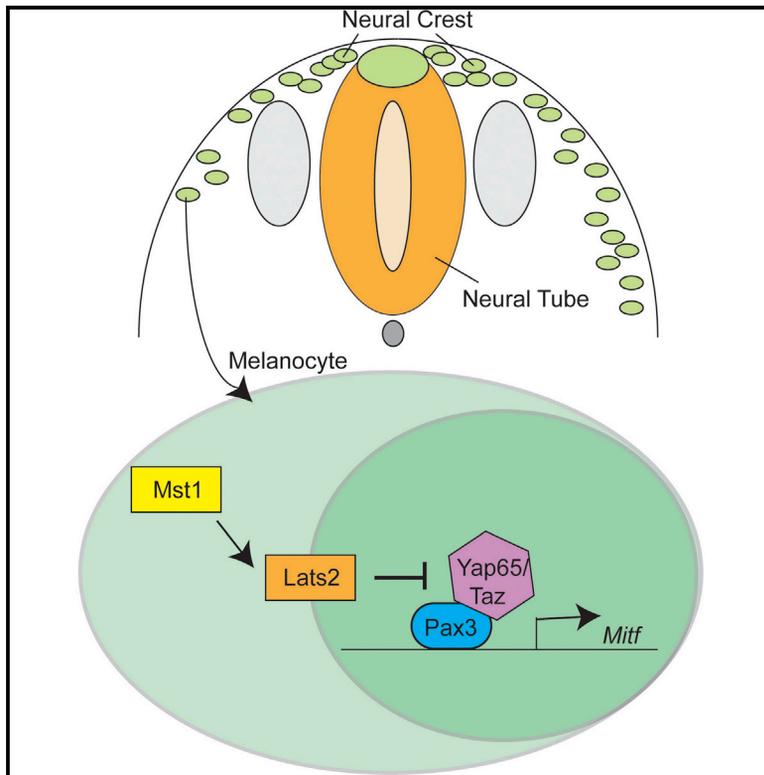
Authors

Lauren J. Manderfield, Kurt A. Engleka, ...,
Eric N. Olson, Jonathan A. Epstein

Correspondence

epsteinj@mail.med.upenn.edu

In Brief

Hippo signaling is a conserved kinase cascade that mediates transcription through a Yap65/Taz-Tead complex and governs organ size. Manderfield et al. have identified Yap65 and Taz as coactivators of Pax factors and established neural crest as a novel site of Hippo signaling. The Pax3-Yap65/Taz complex is regulated by upstream Hippo kinases and is Tead independent. Deletion of Yap65 and Taz in neural crest generated differentiation defects in specific neural crest derivatives.

CrossMark

CellPress

Article

Pax3 and Hippo Signaling Coordinate Melanocyte Gene Expression in Neural Crest

Lauren J. Manderfield,[1] Kurt A. Engleka,[1] Haig Aghajanian,[1] Mudit Gupta,[1] Steven Yang,[1] Li Li,[1] Julie E. Baggs,[2] John B. Hogenesch,[2] Eric N. Olson,[3] and Jonathan A. Epstein[1,4,*]

[1]Department of Cell and Developmental Biology, University of Pennsylvania, Philadelphia, PA 19104, USA
[2]Department of Pharmacology, University of Pennsylvania, Philadelphia, PA 19104, USA
[3]Department of Molecular Biology, University of Texas Southwestern Medical Center, Dallas, TX 75390, USA
[4]Penn Cardiovascular Institute, University of Pennsylvania, Philadelphia, PA 19104, USA
*Correspondence: epsteinj@mail.med.upenn.edu
http://dx.doi.org/10.1016/j.celrep.2014.10.061

SUMMARY

Loss of Pax3, a developmentally regulated transcription factor expressed in premigratory neural crest, results in severe developmental defects and embryonic lethality. Although Pax3 mutations produce profound phenotypes, the intrinsic transcriptional activation exhibited by Pax3 is surprisingly modest. We postulated the existence of transcriptional coactivators that function with Pax3 to mediate developmental functions. A high-throughput screen identified the Hippo effector proteins Taz and Yap65 as Pax3 coactivators. Synergistic coactivation of target genes by Pax3-Taz/Yap65 requires DNA binding by Pax3, is Tead independent, and is regulated by Hippo kinases Mst1 and Lats2. In vivo, Pax3 and Yap65 colocalize in the nucleus of neural crest progenitors in the dorsal neural tube. Neural crest deletion of Taz and Yap65 results in embryo-lethal neural crest defects and decreased expression of the Pax3 target gene, *Mitf*. These results suggest that Pax3 activity is regulated by the Hippo pathway and that Pax factors are Hippo effectors.

INTRODUCTION

Neural crest is a multipotent population of cells arising from the embryonic dorsal neural tube. Following neural tube closure, neural crest cells undergo an epithelial-mesenchymal transition (EMT), migrate along defined routes, and contribute to multiple organs and tissues including craniofacial cartilage, bone, and the pigmented cells of the skin (melanocytes). Neural crest induction is dependent upon inductive signals from neighboring tissues. Wnt and Bmp signaling has been implicated in this process, though the precise details of how inductive signals result in EMT, migration, and cell specification remain to be elucidated.

Pax3 plays a critical role in premigratory neural crest and is thought to orchestrate neural crest-specific gene expression (Goulding et al., 1991). Mutation of Pax3 in the mouse results

in embryonic lethality and a wide array of neural crest abnormalities, including pigmentation defects and congenital heart disease. In the melanocyte lineage, Pax3 functions with Sox10 to directly activate the expression of microphthalmia-associated transcription factor (*Mitf*), which is required for melanogenesis. In humans, *PAX3* mutations result in Waardenburg syndrome, characterized by pigmentation defects and deafness due to neural crest deficiencies.

Other members of the Pax family, consisting of nine related factors in mammals, are expressed in various organs and tissues, where they play critical roles in organogenesis. Pax transcription factors are characterized by the presence of a DNA-binding domain termed the paired domain that mediates sequence-specific protein-DNA interactions (Chi and Epstein, 2002). Although *Pax* genes also encode a C-terminal transactivation domain, in vitro assays reveal relatively weak intrinsic activation capacity. The transactivation potential of Pax factors may be modulated by interacting proteins. For example, a Pax3/Pax7 binding protein, Pax3/7BP, can recruit H3K4 histone methyltransferase activity to Pax target genes in C2C12 myoblasts, thus regulating cell proliferation and the expression of the Pax target genes *Id3* and *Cdc20* (Diao et al., 2012). Pax6 can interact with homeodomain-interacting protein kinase 2 (Hipk2). Hipk2 phosphorylates Pax6 and enhances Pax6 interaction with p300, thereby increasing transcriptional activation (Kim et al., 2006). However, the functional role of Pax interacting factors has not been examined in detail in vivo.

The Hippo signaling pathway is a kinase cascade, initially identified in *Drosophila*, that governs overall organ size through regulation of proliferation and apoptosis (Justice et al., 1995; Xu et al., 1995; Tapon et al., 2002; Harvey et al., 2003; Wu et al., 2003). Following the identification in *Drosophila*, mammalian Hippo signaling molecules have been defined. The upstream kinases Mst1 and Mst2 interact with a scaffolding protein Salvadore1. Mst1 and Mst2 phosphorylate the downstream kinases Lats1 and Lats2 along with associated scaffolding proteins Mobkl1A/Mobkl1b. Lats1 and Lats2 phosphorylate downstream effector molecules of the Hippo pathway, Taz and Yap65. When Hippo signaling is inactive, Taz and Yap65 are dephosphorylated, located in the nucleus, and act as transcriptional coactivators. Canonical transcriptional activation is achieved through association with Tead factors that serve as the DNA-binding
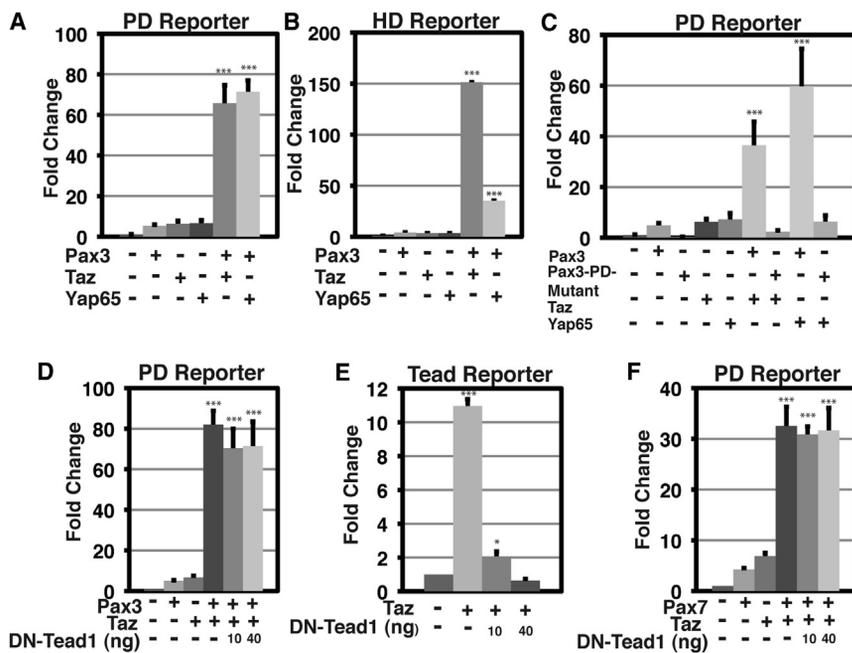
Figure 1. Pax3 Transcriptional Activity Is Significantly Increased in the Presence of Taz or Yap65, and the Activation Is Tead1 Independent

(A) Results of dual luciferase reporter assays in HEK293T cells with Pax3-PairedDomain (PD)-luciferase reporter in the presence (+) or absence (−) of Pax3, Taz, or Yap65.

(B) Results of dual luciferase reporter assays in HEK293T cells with Pax3-HomeoDomain (HD)-luciferase reporter in the presence (+) or absence (−) of Pax3, Taz, or Yap65.

(C) Results of dual luciferase reporter assays in HEK293T cells with Pax3-PD-luciferase reporter in the presence (+) or absence (−) of Pax3, Pax3-PD Mutant, Taz, or Yap65.

(D) Results of dual luciferase reporter assays in HEK293T cells with Pax3-PD-luciferase reporter in the presence (+) or absence (−) of Pax3, Taz, or the specified nanogram amount of DN-Tead1.

(E) Results of dual luciferase reporter assays in HEK293T cells with 8xGTIIC-luciferase reporter in the presence (+) or absence (−) of Taz or the specified nanogram amount of dominant-negative Tead1 (DN-Tead1).

(F) Results of dual luciferase reporter assays in HEK293T cells with Pax3-PD-luciferase reporter in the presence (+) or absence (−) of Pax7, Taz, or the specified nanogram amount of DN-Tead1.

In all experiments, luciferase activity was first normalized to the activity of a cotransfected renilla luciferase construct, then to the activity observed in the absence of specified cDNAs (lane 1). All experiments were performed in duplicate on a minimum of three individual occasions. Data depicted are the mean + SEM. Statistics were completed using an ANOVA with a Tukey-Kramer post hoc comparison test. ***$p < 0.001$, *$p < 0.05$.

partners for Taz and Yap65. Following activation of the Hippo pathway, Taz and Yap65 are phosphorylated and sequestered in the cytoplasm, thus abrogating transcriptional coactivation. In addition to Tead factors, Taz and Yap65 are capable of interacting in vitro with other proteins including Runx2, ErbB4, p63/p73, Tbx5, and Smad-1/2/3/7 (Zaidi et al., 2004; Komuro et al., 2003; Strano et al., 2001; Alarcón et al., 2009; Murakami et al., 2005, Varelas et al., 2008; Ferrigno et al., 2002). We and others have previously shown that Taz/Yap65, via interaction with Tead, can contribute to regulation of *Pax3* gene expression in premigratory neural crest (Milewski et al., 2004; Degenhardt et al., 2010; Gee et al., 2011), and Taz was also identified as a Pax3-interacting protein in a yeast two-hybrid assay (Murakami et al., 2006). Interestingly, Hippo signaling has been shown to promote cellular proliferation and EMT (Lei et al., 2008), two processes critical for the in vivo function of neural crest.

In this article, we demonstrate a potent, synergistic activation of target genes by Pax3 and Taz/Yap65. Target gene activation requires an intact Pax3 DNA-binding domain and is Tead independent. Hippo kinases, Mst1 and Lats2, can inhibit the transcriptional activity of the complex, demonstrating a role for Hippo signaling. Pax3 and Yap65 are coexpressed in the dorsal neural tube at the time of neural crest delamination. Loss of Taz/Yap65 in these premigratory neural crest cells results in downregulation of *Mitf*, a target of coordinated Pax-Hippo signaling. Other members of the Pax family are also coactivated by Taz/Yap65, suggesting that one output of Hippo signaling is activation of Pax targets.

RESULTS

A High-Throughput Screen Identifies Taz and Yap65 as Pax3 Coactivators

To identify potential Pax3 coactivator molecules, we conducted a high-throughput screen by cotransfecting a Pax3 expression plasmid along with a Pax3 luciferase reporter vector with each of ~15,000 human and mouse cDNAs arrayed in 384-well plates in human embryonic kidney 293T (HEK293T) cells (Mammalian Gene Collection MGCv1 library, Open BioSystems). The Pax3 reporter contains five Pax3 paired-domain DNA binding sequences (Epstein et al., 1994) upstream of a synthetic minimal promoter directing firefly luciferase expression. Potential Pax3 coactivators were identified as cDNAs that generated luciferase activity greater than that of Pax3 alone. Both Taz and Yap65 were identified among the top five coactivators (Table S1). We confirmed that Pax3 can interact with Yap65, like Taz (Murakami et al., 2006), using the Duolink system, which utilizes a proximity ligation assay to monitor protein-protein interactions in situ (Figure S1A). Independent validation experiments in HEK293T cells confirmed the ability of either Taz or Yap65 to induce synergistic transactivation of the synthetic Pax3 luciferase reporter when transfected with Pax3 (Figure 1A). When Pax3, Taz, or Yap65 was expressed independently, each induced only ~4- to 5-fold activation. In contrast, when Pax3 was coexpressed with either Taz or Yap65, over 60-fold activation was induced (Figure 1A). The nine mammalian Pax genes can be divided into four families based upon sequence conservation, and members of each Pax subfamily can function synergistically with Taz and Yap65 (Figure S1).

Several Pax family members, including Pax3, contain a homeodomain DNA binding domain in addition to the paired domain, and Pax3 can occupy both paired and homeodomain recognition motifs in vivo (Soleimani et al., 2012). To determine if the presence of Taz or Yap65 enhances Pax3 activation at homeodomain sequences, we generated a Pax-homeodomain luciferase reporter containing nine Pax homeodomain DNA binding motifs upstream of a synthetic minimal promoter directing firefly luciferase expression. Pax3 could synergize with either Taz or Yap65 to activate the synthetic homeodomain reporter (Figure 1B).

Pax3-Taz/Yap65 Activation Requires Pax3 DNA Binding and Is Tead Independent

Taz and Yap65 are generally thought to act by interacting with Tead factors, which are expressed ubiquitously, although alternative DNA binding proteins have been described to interact with Taz or Yap65 in vitro (Zhang et al., 2009; Zhao et al., 2008; Zaidi et al., 2004; Komuro et al., 2003; Strano et al., 2001; Murakami et al., 2006). To establish if DNA binding by Pax3 is required for transcriptional coactivation observed in our assays, we examined the effect of a missense mutation in the Pax3 paired domain found in a patient with Waardenburg syndrome that impairs sequence-specific DNA interactions (Epstein et al., 1995). The Pax3 DNA binding mutant (Pax3-PD Mutant) was unable to synergize with either Taz or Yap65 (Figure 1C). These data suggest that Pax3 must associate with DNA to mediate the robust activation observed in the presence of Taz and/or Yap65. The Pax3-PD Mutant was able to synergize with Taz or Yap65 when a homeodomain reporter was used and protein expression was confirmed by immunoblot (Figure S2). Furthermore, inhibition of Tead activity by expression of a dominant-negative Tead mutant (DN-Tead1) consisting of a truncated protein that retains DNA-binding capacity but cannot recruit Taz (Zhang et al., 2009; Zhao et al., 2008) failed to prevent Pax3 synergy with Taz (Figure 1D), although it efficiently abolished Taz activation of a Tead-dependent reporter (Figure 1E). Pax7, which is closely related to Pax3 and is coexpressed in the dorsal neural tube, can also synergize with Taz in a Tead-independent manner (Figure 1F). Thus, we infer that Taz and Yap65 can act as direct coactivators of Pax3/7 target genes.

Pax3 and Yap65 Colocalize in the Dorsal Neural Tube

Pax3 is actively transcribed in the dorsal neural tube during early/midgestation (approximately embryonic day 8 [E8] to E10) when neural crest cells undergo an epithelial-to-mesenchymal transition, delaminate, and migrate throughout the body (Goulding et al., 1991). Yap65 is ubiquitously expressed at similar stages (Morin-Kensicki et al., 2006). At E9.5 we observed Pax3 and Yap65 nuclear colocalization in the dorsal neural tube (Figure 2), dorsal root ganglia, which is derived from the neural crest (Figure 2A, asterisk), and somites (Figure 2H). Within the dorsal neural tube, Pax3 and Yap65 are colocalized in the dorsalmost aspect, the site at which neural crest cells undergo EMT and delaminate prior to migration. At E10.5 (Figures 2E–2G) and E11.5 (Figures 2I–2K), phosphorylated Yap65 becomes prominent (Figures 2G and 2K) and nuclear Yap65 is greatly reduced (Figures 2F and 2J), indicating activation of Hippo signaling. Thus, Pax3 and Yap65 are colocalized in the nucleus of premigratory neural crest cells.

Loss of Taz and Yap in Neural Crest Results in Craniofacial Defects and Downregulation of Mitf

To examine the biological significance of Taz and Yap65 in the neural crest, floxed alleles were utilized to delete *Taz* and *Yap65* in premigratory neural crest using *Wnt1-Cre* (Xin et al., 2011, 2013). Genotyping of 76 postnatal day 10 (P10) pups resulting from *Wnt1-Cre; Taz^{flox/+};Yap^{flox/+}* x *Taz^{flox/flox};Yap^{flox/flox}* crosses identified no surviving *Wnt1-Cre;Taz^{flox/flox};Yap^{flox/flox}* or *Wnt1-Cre;Taz^{flox/+};Yap^{flox/flox}* mice and five of nine surviving *Wnt1-Cre;Taz^{flox/flox};Yap^{flox/+}* mice had craniofacial defects (Table 1). Further analysis of genotype frequencies at various stages of gestation indicated that *Wnt1-Cre;Taz^{flox/flox};Yap^{flox/flox}* embryos undergo fetal demise prior to E11.5, although they were identified at the expected frequency at E9.5 (Table 1) when they appeared grossly normal (Figures 3A–3D). At E10.5, 13 of 13 *Wnt1-Cre;Taz^{flox/flox};Yap^{flox/flox}* embryos exhibited overt craniofacial defects (Table 1; Figure 3). Within the neural tubes of the E10.5 Yap65/Taz deletion embryos, there was no detectable change in the percentage of proliferating or apoptotic cells (Figure S3). Grossly, hemorrhages were evident in the branchial arch regions in the Yap65/Taz double-null embryos (Figures 3Q and 3R). Histologic analysis revealed deficiencies of facial mesenchyme in the maxillary and mandibular branchial arches (Figures 3S and 3T), regions normally populated by neural crest. Deletion of both Yap65 alleles and a single Taz allele resulted in a similar hemorrhagic phenotype (Figures 3M and 3N), although facial mesenchyme appeared intact (Figures 3O and 3P), and mice of this genotype were not identified postnatally (Table 1). In embryos in which both *Taz* alleles and a single *Yap65* allele were removed, the embryos were phenotypically normal at E10.5 (Figures 3I–3L) and they survived postnatally (Table 1).

We followed the fate of neural crest cells with or without Yap65 and Taz by including a *R26tdTomato* (*R26^{Tom/+}*) Cre reporter allele. Wnt1-derived cells can be identified in resultant embryos by expression of tdTomato and detection with an anti-red fluorescent protein antibody. Examination of control and double-mutant embryos at E10.5 showed that neural crest migration was grossly intact (Figure 4). Neural crest derivatives populated the branchial arches and peripheral ganglia (Figures 4B and 4E), and Pax3 expression was maintained in double-null embryos (Figures 4C and 4F). Serial sections of fate-mapped E10.5 embryos revealed intact migration of neural crest throughout the embryo, where they populated regions of presumptive facial mesenchyme, the peripheral nervous system, and the enteric ganglia (Figures 4G, 4H, 4L, and 4M). Neurofilament expression by neural crest-populating peripheral ganglia appeared normal, as determined by costaining of fate-mapped neural crest cells with the 2H3 anti-neurofilament antibody (Figures 4I, 4J, 4N, and 4O). Enteric ganglia derivatives expressed Sox10 at levels indistinguishable from controls (Figures 4K and 4P). Thus, many aspects of neural crest migration and fate specification appeared intact despite the loss of Taz/Yap65.

Mitf Is Coordinately Regulated by Pax3 and Yap/Taz

Neural crest-derived cells were also observed adjacent to surface ectoderm in both control and double null-embryos where migrating melanoblasts are normally found (Figures 5A and 5B). In control embryos, these cells expressed Mitf, a transcriptional

| Pax3 | Yap (nuclear) | pYap | Merge (E9.5) |
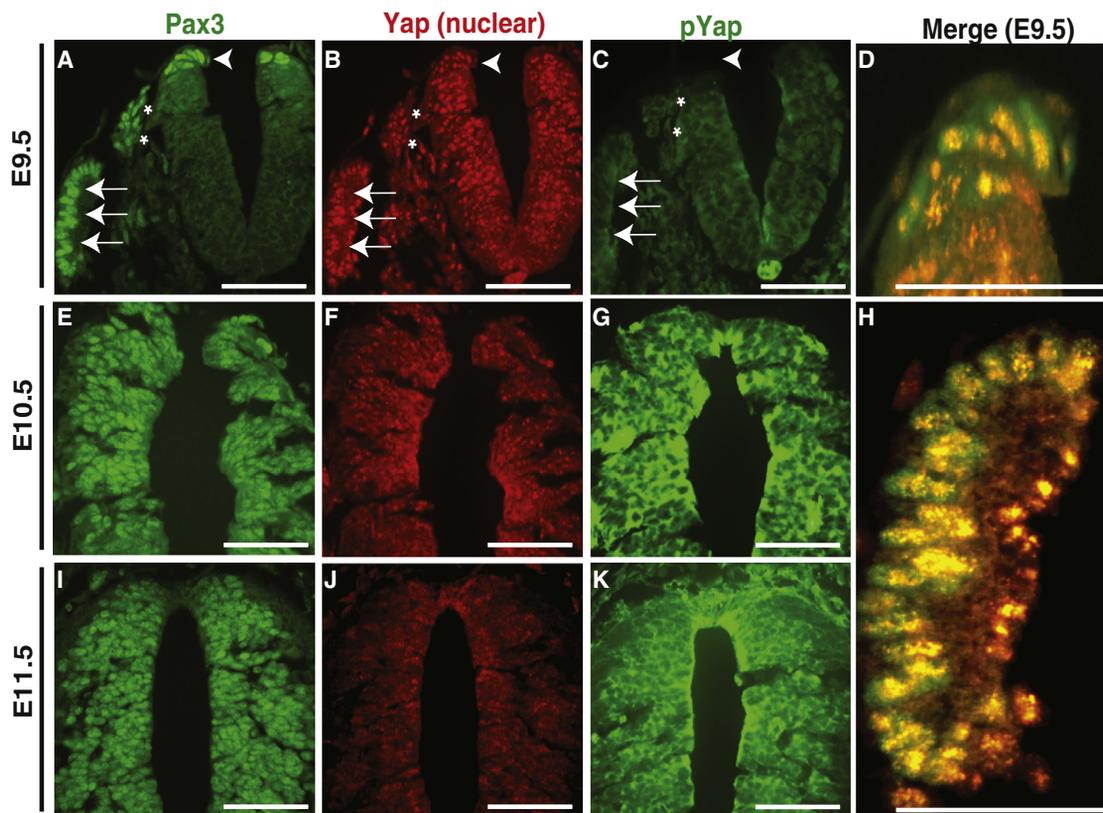
Figure 2. Pax3 and Yap65 Are Coexpressed in the Dorsal Neural Tube at E9.5

(A–D and H) Frontal sections of E9.5 wild-type embryos.

(E–G) Frontal sections of E10.5 wild-type embryos.

(I–K) Frontal sections of E11.5 wild-type embryos.

(A), (E), and (I) display immunostaining for Pax3. (B), (F), and (J) depict immunostaining for Yap65. (C), (G), and (K) display immunostaining for phospho-Yap. At E9.5 (A and B), Pax3 and Yap are colocalized in the dorsal neural tube (arrowhead), dorsal root ganglion (asterisks), and somites (arrows). Higher-magnification Pax3/Yap merged images of the dorsal neural tube (D) and somite (H) display the high level of overlap of Pax3 and Yap. In (A)–(C), (E)–(G), and (I)–(K), scale bars represent 100 μm. In (D) and (H), scale bars represent 50 μm.

activator of melanogenesis regulated by Pax3 (Watanabe et al., 1998) (Figure 5A). However, in double-knockout embryos, Mitf expression was markedly downregulated in these neural crest derivatives (Figure 5B). Quantitation of red fluorescent protein (RFP)/Mitf-positive cells adjacent to and within the surface ecto-derm revealed a significant decrease in the percentage of RFP+ cells that also expressed Mitf in Yap65/Taz null embryos (Figure 5C). In mouse embryonic fibroblasts derived from $Taz^{flox/flox}$; $Yap^{flox/flox}$ embryos, treatment with a Cre virus to delete both alleles of Yap65 and Taz produced a significant decrease in Mitf expression (Figure 5D). Dopachrome tautomerase (Dct) is a direct transcriptional target of Mitf (Lang et al., 2005) and was similarly decreased following deletion of Yap65 and Taz (Figure 5D). We sought to determine if altered Mitf expression in Yap/Taz double-knockout embryos was due to loss of synergy between Pax3 and Yap/Taz or if this was a result of Tead-dependent Yap/Taz gene regulation. Regulatory elements controlling Mitf expression have been extensively characterized previously (Watanabe et al., 1998; Bondurand et al., 2000; Potterf et al., 2000). Both Pax3 and Pax7 can synergize with Taz and Yap65 to activate a Mitf-luciferase reporter construct (Figures 5F and

5G). Although 18 potential Tead binding sites are located in the Mitf promoter/enhancer region included in this assay (Figure 5E), DN-Tead1 failed to significantly impair synergistic Pax-Taz/Yap65 coactivation (Figures 5H and 5I), suggesting that Mitf activation by Pax3 and Taz is Tead independent.

Two Pax3 paired-domain binding sites have been described within this Mitf enhancer: site P1 at position −260 to −244 and site P2 at position −40 to −26 upstream of the transcription start site (Watanabe et al., 1998; Bondurand et al., 2000; Potterf et al., 2000). Sequence analysis utilizing the TRANSFAC database identified an additional previously uncharacterized potential Pax3 binding site, which we termed P3, located at position −160 to −143 relative to the transcription start site. A 519 bp fragment of the Mitf enhancer, which contains the P1, P2, and P3 sites, retained the ability to be synergistically activated by Pax3 with Taz or Yap65 with activity comparable to the full-length Mitf reporter (Figure S4). Each Pax3 binding site was then evaluated individually in ~100–200 bp Mitf promoter/enhancer fragments. Fragments containing P2 and P3 exhibited coactivation with Taz and Yap65, but the coactivation at site P1 was not significant in the context of the enhancer fragment.

Table 1. Genotyping Results of the Wnt1-Cre;Taz$^{flox/+}$;Yap$^{flox/+}$ x Taz$^{flox/flox}$;Yap$^{flox/flox}$ Cross

| Age | Genotype Wnt1-Cre;Taz$^{flox/+}$;Yap$^{flox/+}$ x Taz$^{flox/flox}$;Yap$^{flox/flox}$ Cross | | | | | | | | Total | χ^2 |
	Taz$^{flox/+}$; Yap$^{flox/+}$	Taz$^{flox/flox}$; Yap$^{flox/+}$	Taz$^{flox/+}$; Yap$^{flox/flox}$	Taz$^{flox/flox}$; Yap$^{flox/flox}$	Wnt1-Cre; Taz$^{flox/+}$; Yap$^{flox/+}$	Wnt1-Cre; Taz$^{flox/flox}$; Yap$^{flox/+}$	Wnt1-Cre; Taz$^{flox/+}$; Yap$^{flox/flox}$	Wnt1-Cre; Taz$^{flox/flox}$; Yap$^{flox/flox}$		
E9.5	14	7	8	12	8	8	8	8	73	N/S
E10.5	5	7	10	4	7	7	4	13[a]	57	N/S
E11.5	5	10	8	2	9	6	7	0	47	0.0493
P10	12	8	14	18	15	9[b]	0	0	76	0.0001

N/S, not significant.
[a]Craniofacial abnormalities (13/13)
[b]Craniofacial hemorrhage (5/9)

Mutation of the Pax3 binding sites within P2 and P3 led to a statistically significant decrease in the observed coactivation with Taz and Yap65. The P2 and P3 fragments each contain a single predicted Tead binding site, but DN-Tead1 did not significantly decrease Pax3-Taz or Pax3-Yap65 coactivation of the P2, P3, or 519 bp *Mitf* reporter (Figure S5). Taken together, we interpret these results to indicate that P2 and P3, but not P1, act as docking sites for a Pax3-Taz/Yap65 coactivation complex.

Hippo Kinases Mst1 and Lats2 Can Inhibit Pax3-Taz/Yap65 Synergistic Activation

Taz and Yap65 are downstream effectors of the Hippo signaling pathway that is composed of a series of regulatory protein kinases, including Mst and Lats. Activation of the Hippo pathway culminates in phosphorylation of Taz/Yap65, which induces translocation to the cytoplasm and abrogation of nuclear functions. Serine residue 89 of the Taz protein was previously demonstrated to be a critical residue for Lats kinase phosphorylation (Lei et al., 2008). Upon mutation to alanine, TazS89A gains resistance to Lats regulation and is constitutively nuclear (Lei et al., 2008). When Pax3 was coexpressed with TazS89A, there was over 130-fold activation of a Pax3 reporter (Figure 6A), consistent with constitutive activation. TazS89A was even more potent than wild-type Taz, suggesting basal activity of Hippo signaling under these experimental conditions.

We probed the ability of upstream Hippo kinases Mst1 and Lats2 to modulate Pax3-Taz/Yap65 transcriptional synergy. Both Mst1 and Lats2 inhibited Pax3-Taz and Pax3-Yap65 coactivation (Figures 6B–6E). Kinase inactive mutants of Mst1 or Lats2, Mst1KI (Mst1-K59R) or LATS2KI (LATS2-D809A), respectively, were relatively ineffective at inhibiting Pax3-Taz and Pax3-Yap65 coactivation (Figures 6B–6E). Immunoblot analysis confirmed that the wild-type and kinase inactive forms of each Hippo kinase were expressed at equivalent protein levels (Figures 6F and 6G). LATS2 also significantly inhibited coactivation of the endogenous *Mitf* enhancer by Pax3-Taz/Yap65 (Figures 6H–6I). In contrast, expression of LATS2KI did not alter Pax3-Taz or Pax3-Yap65 coactivation at the *Mitf* enhancer (Figures 6H and 6I). Thus, transcriptional synergy between Pax factors and Yap/Taz can be modulated by upstream regulators of the Hippo pathway.

We further examined the ability to Pax3 and Pax7 to coactivate another previously described Pax target gene. Myf5 is a regulator of myogenic determination that is another example of a direct transcriptional target of Pax3/7 (Bajard et al., 2006). Pax3 and Pax7 each functioned with Taz or Yap65 to coactivate a previously described *Myf5* enhancer (Figures S6A–S6C). This activation was Tead independent, as the presence of DN-Tead1 did not alter the coactivation (Figures S6D and S6E). Further Lats2, but not Lats2KI, significantly inhibited Pax3-Taz/Yap65-mediated activation of the *Myf5* reporter (Figures S6F and S6G).

DISCUSSION

Hippo signaling is a critical regulator of proliferation and EMT during development and in cancer (Lei et al., 2008). In this study, we demonstrate that the downstream effector molecules of Hippo signaling, Taz and Yap65, can function as coactivators of Pax3. This complex requires Pax3 to act as the DNA binding moiety and is regulated by upstream Hippo kinases. Unlike canonical Hippo signaling, the Pax3-Taz/Yap65 complex does not require Tead factors to mediate activity. Deletion of Taz and Yap65 in premigratory neural crest resulted in craniofacial defects, similar to those seen in the absence of Pax3 and Pax7 (Mansouri and Gruss, 1998), and downregulation of the Pax3 target, Mitf. In vitro data suggest that another Pax3 target, Myf5, can also be coordinately regulated by Pax3 and Yap/Taz.

It remains unclear if all Pax targets will require Yap65 or Taz for functional activation or if a subset of physiologic target genes are Yap/Taz independent. Clearly, many Yap/Taz targets are Pax independent and rely on Tead factors to mediate DNA binding. It is likely that Pax factors can activate (or repress) some downstream pathways in the absence of Yap/Taz, while a subset of targets are strongly coactivated in the presence of both Pax and Yap/Taz. Further delineation of the various classes of downstream-regulated genes will be important to define the extent of Pax/Hippo coordinate regulation.

The Pax3-Taz/Yap65 complex produces potent transcriptional activation. In vivo, this complex is likely to include additional factors that may vary with context. Candidates include the previously identified Pax3/7 binding protein, Pax3/7BP, which recruits an H3K4 histone methyltransferase to target gene promoters (Diao et al., 2012). Taz has been shown to interact with the histone acetyl transferases PCAF and p300 (Murakami et al., 2005). This interaction greatly enhances Taz
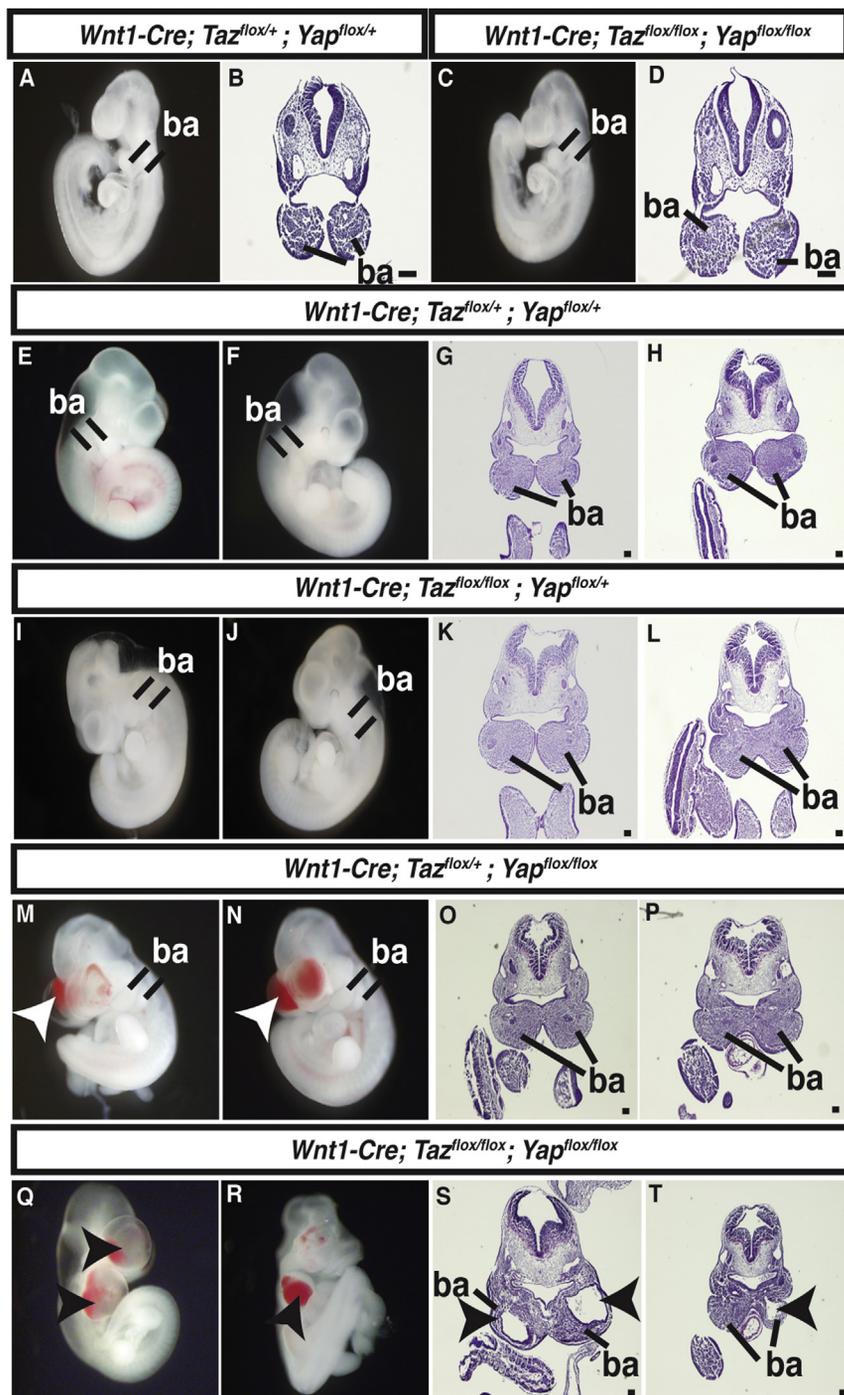
Figure 3. Taz and Yap65 Are Required for Normal Neural Crest Development
Whole-mount bright-field images (A, C, E, F, I, J, M, N, Q, and R) and H&E-stained transverse sections (B, D, G, H, K, L, O, P, S, and T) of representative embryos of the indicated genotypes at E9.5 (A–D) and E10.5 (E–T). Arrowheads in (M), (N), and (Q)–(T) indicate regions of abnormal facial mesenchyme. ba, branchial arches. Scale bars, 100 μm.

example, is critical for formation of the eye and is mutated in inherited causes of blindness. Pax2 functions in early kidney formation, Pax8 functions in the thymus and has also been shown to coactivate with Taz, and Pax1/9 functions in the skeleton (Di Palma et al., 2009). Hippo signaling is known to regulate organ size. The functional interaction of Pax proteins with Yap65 and Taz may provide a physical and functional mechanism to link organogenesis with the regulation of organ size. Likewise, disruption of Pax function has been implicated in cancer, and the role of Pax/Hippo synergy in oncogenesis will be an important area of future investigation.

EXPERIMENTAL PROCEDURES

Plasmids

The firefly-luciferase reporter construct 5xPax3BS was provided by M. Buckingham (Relaix et al., 2003) and subcloned into pGL4.27 (Promega). To generate a Pax3-homeodomain reporter construct, a previously identified Pax homeodomain-binding motif (Soleimani et al., 2012), TAATT-GATTA, was synthetically generated and reiterated nine times. This sequence was then cloned upstream of pGL4.27 for use in luciferase assays (Promega). An *MITF* reporter previously published, containing approximately 2 kb of the 5′ proximal human promoter (chr3:69,934,337-69,936,682 [hg38]; Lang et al., 2005) was subcloned into pGL4.27 (Promega). 8xGTIIC, a Tead reporter, was provided by S. Piccolo (Dupont et al., 2011; Addgene plasmid 34615). Murine *Taz* and *Taz-S89A* expression vectors were described previously (Kanai et al., 2000; Addgene plasmids 19025 and 19026) and were subcloned into pCMV-Sport6 (Invitrogen). Murine *Yap65* was expressed in pCMV-Sport6 (Invitrogen) as described previously (Milewski et al., 2004). Dominant-negative human *TEAD1* (*DN-TEAD1*) was provided by Kun-Liang Guan (Zhang et al., 2009; Zhao et al., 2008). Murine hippo kinases *Mst1* and *Mst1-KI* were previously described (Lin et al., 2002; Addgene plasmids 1965 and 1966). Expression plasmids for human hippo kinases *LATS2* and *LATS2-KI* were provided by D. Pan (Dong et al., 2007). The murine *Pax3* expression construct was previously described (Lang et al., 2000) and was subcloned into pCMV-Sport6 (Invitrogen). The murine Pax3 paired-domain mutant (*Pax3-PD Mutant*) contains a single cytosine to thymine mutation that produces a proline to leucine change at amino acid 50, which prevents Pax3 binding to DNA sequences,

transcriptional activity at an atrial natriuretic factor promoter reporter construct (Murakami et al., 2005). Future studies will elucidate the nature of additional Pax/Taz/Yap complex subunits.

Since Pax factors from all Pax families can utilize Taz and Yap65 as coactivators, Hippo signaling could be a common means to regulate activity of many Pax target genes in diverse developmental contexts. Pax genes function in multiple developing tissues and play key roles in organogenesis. Pax6, for
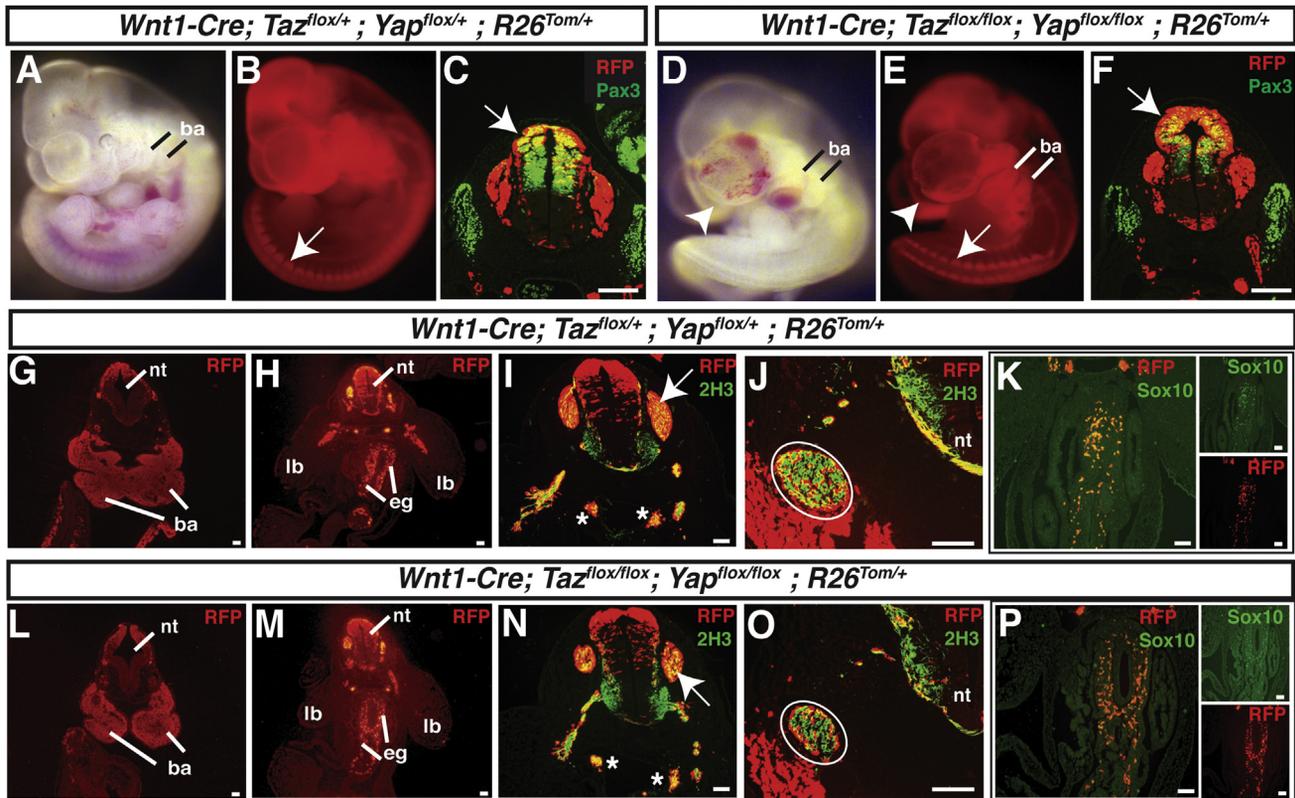
Figure 4. Characterization of Embryos Lacking Taz and Yap65

(A and B) *Wnt1-Cre; Taz flox/+ ;Yap flox/+; R26Tom/+* E10.5 embryo imaged in bright field (A) and fluorescence (B).

(C) Transverse sections of E10.5 *Wnt1-Cre; Taz flox/+ ;Yap flox/+; R26Tom/+* embryo stained tdTomato (RFP) and Pax3.

(D and E) *Wnt1-Cre; Taz flox/flox;Yap flox/flox; R26Tom/+* E10.5 embryo imaged in bright field (D) and fluorescence (E).

(F) Transverse sections of E10.5 *Wnt1-Cre; Taz flox/flox;Yap flox/flox; R26Tom/+* embryo stained for tdTomato (RFP) and Pax3.

(G–K) Transverse sections of E10.5 *Wnt1-Cre; Taz flox/+ ;Yap flox/+;R26Tom/+* embryos stained for tdTomato (RFP) (G and H), tdTomato (RFP) and neurofilament (2H3) (I and J), or tdTomato (RFP) and Sox10 (K).

(L–P) Transverse sections of E10.5 *Wnt1-Cre; Taz flox/flox ;Yap flox/flox;R26Tom/+* embryos stained for tdTomato (RFP) (L and M), tdTomato (RFP) and neurofilament (2H3) (N and O), or tdTomato (RFP) and Sox10 (P).

Arrows in (C) and (F) designate costaining in the dorsal neural tube. Branchial arches (ba) are invested with red-fluorescing Wnt1-derived neural crest (A, B, D, and E). Arrows in (I) and (N) mark dorsal root ganglia, while asterisks demark the right and left sympathetic trunks. Circled areas in (J) and (O) denote the glosso-pharyngeal (IX) preganglion. ba, branchial arches; lb, limb bud; nt, neural tube; eg, enteric ganglia. Images were merged after global adjustment for brightness and were produced by combining respective red and green channels using Photoshop software (Adobe). Scale bars, 100 μm.

was previously described (Epstein et al., 1995) and was subcloned into pCMV-Sport6 (Invitrogen). Human *PAX7* was expressed in pcDNA3 (Invitrogen).

Cell Culture and Luciferase Assay

HEK293T cells were maintained at 37°C with 5% CO_2 in Dulbecco's modified Eagle's medium supplemented with 10% fetal bovine serum, penicillin, and streptomycin. All HEK293T cell transfections were completed using FuGene6 (Roche). Experiments utilized 250 ng of the specified firefly-luciferase reporter constructs, 80 ng *Taz/Yap65*, 40 ng Pax expression vector, and 75 ng pGL2-Basic-renilla luciferase (Promega). In experiments with *Mst1*, *Mst1-KI*, *LATS2*, or *LATS2-KI*, 120 ng of the kinase expression vector was included. All transfections maintained an equal concentration of total DNA with the inclusion of the pCMV-Sport6 empty vector (Invitrogen). Cellular extracts were collected 48 hr posttransfection for use in a dual-luciferase assay (Promega). Twenty microliters of cellular extract was used to assess firefly and renilla luciferase activities and luciferase activity was normalized to the renilla activity. All experiments were performed in duplicate on at least three separate occasions. Statistical differences between conditions were analyzed using ANOVA, with a Tukey-Kramer post hoc comparison test.

Western Blot

HEK293T cells were transfected with 2 μg of the specified Hippo kinase: *Mst1*, *Mst1KI*, *LATS2*, *LATS2-KI*. Mst1 and Mst1KI contain an N-terminal FLAG epitope tag, while LATS2 and LATS2KI contain an N-terminal myc epitope tag. A nontransfected plate of cells was processed in parallel as a control. A total of 48 hr posttransfection, cells were lysed in RIPA buffer (150 mm NaCl, 50 mm Tris-Base [pH 7.5], 1% IGEPAL, 0.5% sodium deoxycholate, 0.1% SDS) plus protease inhibitors (Complete Mini, Roche). All lysates were quantitated with a BCA Assay (Promega) and an equal amount of total protein was loaded per well of a 4%–12% gradient gel and run at 120 V for 2 hr. Blots were transferred overnight at 4°C, at 20 V onto a polyvinylidene fluoride membrane (Invitrogen). Membranes were blocked in 10% nonfat dry milk/Tris-buffered saline and Tween 20 and incubated in primary antibody overnight: M2-FLAG (mouse monoclonal, Sigma), myc (mouse monoclonal, Cell Signaling #2276), or actin (rabbit polyclonal, Cell Signaling, #4970). All blots were probed with horseradish peroxidase-conjugated secondary antibody for 1 hr with either anti-mouse secondary (Cell Signaling) or anti-rabbit secondary (Cell Signaling). Blots were developed using ECL Prime (Amersham).
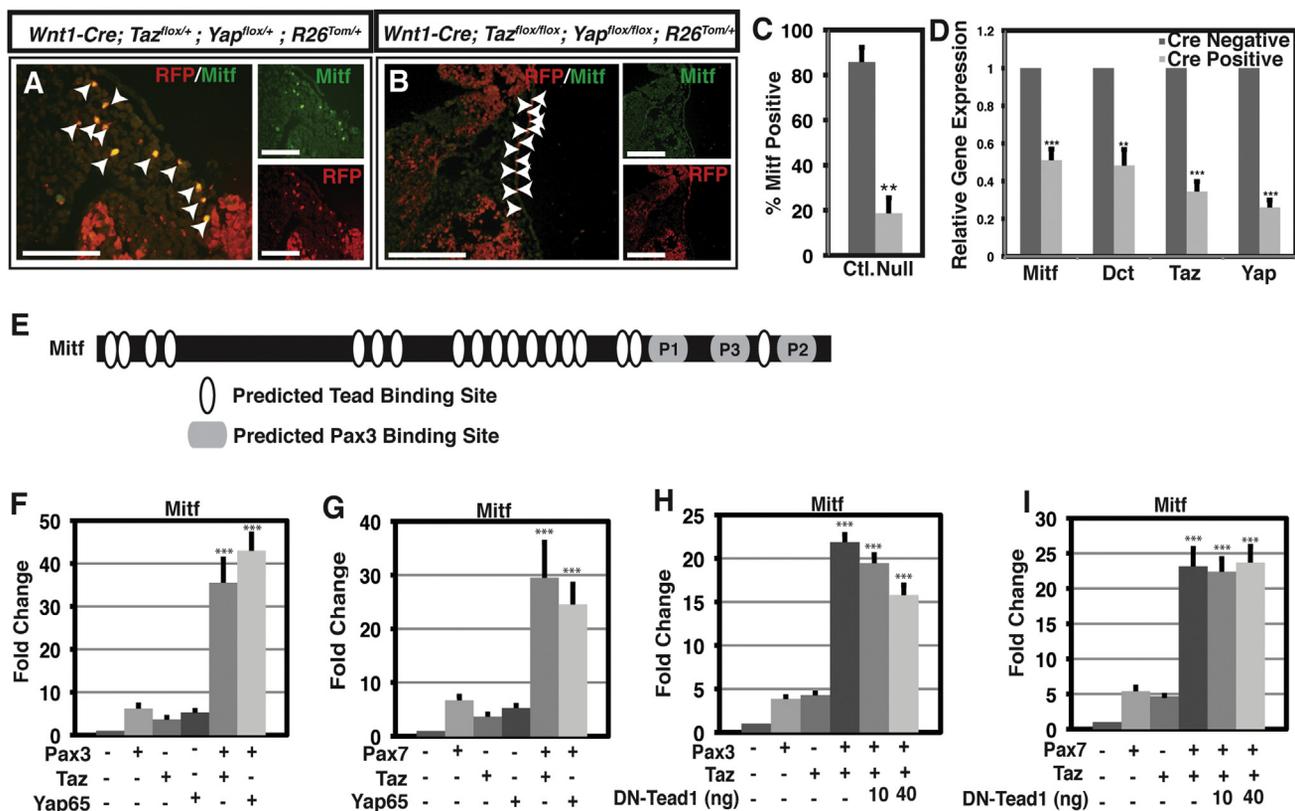
Figure 5. *Mitf* Is Coordinately Regulated by Pax3 and Yap/Taz

(A and B) Fluorescent images of transverse sections of E10.5 embryos immunostained for Mitf and tdTomato (RFP). (A) Colabeled cells adjacent to surface ectoderm where migrating melanoblasts are normally found are indicated by arrowheads. (B) Migratory neural crest cells near the ectoderm that do not express Mitf in double-mutant embryos are indicated by arrowheads. Scale bars, 100 μm.

(C) Quantitation of RFP/Mitf expressing cells adjacent to and in the surface ectoderm of control (Ctl.) and Yap65/Taz double-null embryos (Null). Data depicted are the average percentage of RFP+ cells that also express Mitf + SEM. A minimum of 60 cells were quantified from both control and null animals encompassing sections from three individual control and null embryos. Images were merged after global adjustment for brightness and were produced by combining respective red and green channels using Photoshop software (Adobe).

(D) Quantitative real-time PCR of untreated or Cre-virus treated *Taz^flox/flox^;Yap^flox/flox^* mouse embryonic fibroblasts for *Mitf*, *Dct*, *Taz*, and *Yap65*. Data are the mean + SEM.

(E) Schematic representation of a Mitf luciferase reporter plasmid. Pax3 binding sites are denoted within gray oblong circles. Predicted TEAD binding sites are denoted with white ovals, representing the consensus sequence XDGHATXT, where X = A, T, C, or G; D = A or T; and H = A, T, or C (Anbanandam et al., 2006).

(F) Results of dual luciferase reporter assays in HEK293T cells with Mitf-luciferase reporter in the presence (+) or absence (−) of Pax3, Taz or Yap65.

(G) Results of dual luciferase reporter assays in HEK293T cells with Mitf-luciferase reporter in the presence (+) or absence (−) of Pax7, Taz or Yap65.

(H) Results of dual luciferase reporter assays in HEK293T cells with Mitf-luciferase reporter in the presence (+) or absence (−) of Pax3, Taz or the specified nanogram (ng) amount of DN-Tead1.

(I) Results of dual luciferase reporter assays in HEK293T cells with Mitf-luciferase reporter in the presence (+) or absence (−) of Pax7, Taz or the specified nanogram amount of DN-Tead1.

Statistics in (C) and (D) were completed using a Student's t test (**p < 0.01, ***p < 0.001). In all experiments, luciferase activity was first normalized to the activity of a cotransfected renilla luciferase construct, then to the activity observed in the absence of specified cDNAs (lane 1). All experiments were performed in duplicate a minimum of three individual occasions. Data depicted in (F)–(I) are the mean + SEM. Statistics were completed using an ANOVA with a Tukey-Kramer post hoc comparison test. ***p < 0.001

Histology and Immunofluorescence

Samples were harvested, fixed overnight in 4% paraformaldehyde, and dehydrated through an ethanol series. All samples were paraffin embedded and sectioned. Antibodies used for immunofluorescence were anti-Pax3 mouse monoclonal (developed by C.P. Ordahl and obtained from the Developmental Studies Hybridoma Bank, created by The Eunice Kennedy Shriver National Institute of Child Health and Human Development [NICHD] of the NIH), anti-Yap rabbit polyclonal (Cell Signaling #4912S), anti-phospho-Yap rabbit polyclonal (Cell Signaling #4911), anti-neurofilament (2H3, developed by T. M. Jessell and J. Dodd obtained from the Developmental Studies Hybridoma

Bank, created by the NICHD of the NIH), anti-Mitf (Vector Laboratories, clone 34CA5), anti-Sox10 (Santa Cruz Biotechnology, N-20), and anti-RFP (Rockland Immunochemicals, #600-401-379). Hematoxylin and eosin (H&E) staining was completed using a standard protocol.

Melanocyte Quantitation

Transverse sections from *Wnt1-Cre;Taz^flox/+^;Yap^flox/+^;R26^Tom/+^* and *Wnt1-Cre;Taz^flox/flox^;Yap^flox/flox^;R26^Tom/+^* E10.5 embryos were costained for RFP and Mitf. Cells greater than 100 μm from the surface ectoderm were excluded from analysis. Seven sections from three independent embryos were included
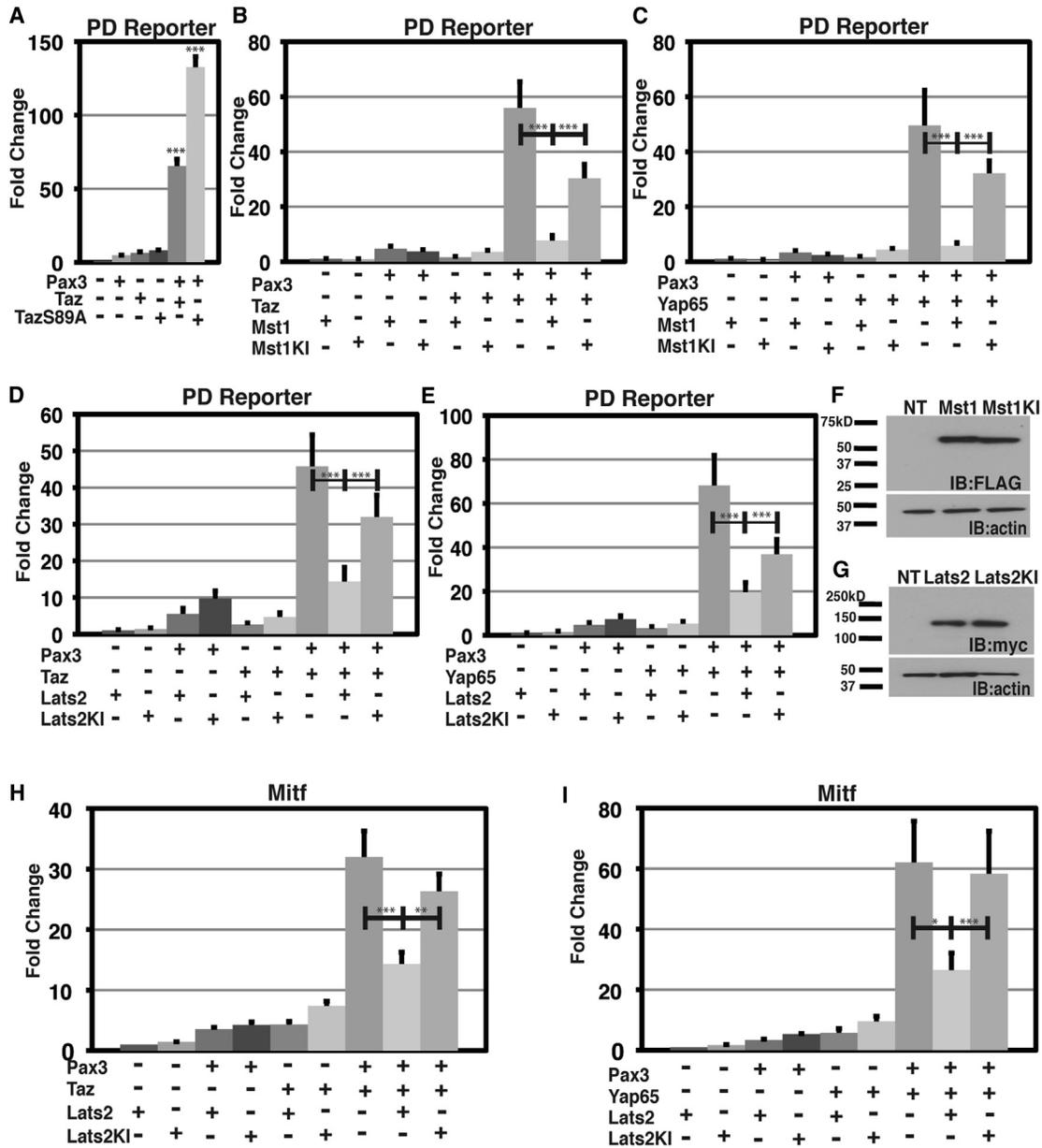
Figure 6. Hippo Kinases Mst1 and Lats2 Can Inhibit the Activity of the Pax3-Taz/Yap Complex

(A) Results of dual luciferase reporter assays in HEK293T cells with Pax3-PD-luciferase reporter in the presence (+) or absence (−) of Pax3, Taz, or constitutively active Taz, TazS89A.

(B) Results of dual luciferase reporter assays in HEK293T cells with Pax3-PD-luciferase reporter in the presence (+) or absence (−) of Pax3, Taz, Mst1, or a kinase-inactive form of Mst1, Mst1KI.

(C) Results of dual luciferase reporter assays in HEK293T cells with Pax3-PD-luciferase reporter in the presence (+) or absence (−) of Pax3, Yap65, Mst1, or Mst1KI.

(D) Results of dual luciferase reporter assays in HEK293T cells with Pax3-PD-luciferase reporter in the presence (+) or absence (−) of Pax3, Taz, Lats2, or Lats2KI.

(E) Results of dual luciferase reporter assays in HEK293T cells with Pax3-PD-luciferase reporter in the presence (+) or absence (−) of Pax3, Yap65, Lats2, or Lats2KI.

(F) Anti-FLAG western blot from HEK293T cells either nontransfected (NT) or transfected with a FLAG-tagged Mst1 or FLAG-tagged Mst1KI. Western blots of the same cellular protein lysates were also probed with anti-actin to demonstrate equivalent protein loading among samples.

(G) Anti-myc western blot from HEK293T cells either nontransfected (NT), transfected with a myc-tagged Lats2, or transfected with a kinase-inactive form of Lats2, a myc-tagged Lats2KI. Western blots of the same cellular protein lysates were also probed with anti-actin to demonstrate equivalent protein loading among samples.

(H) Results of dual luciferase reporter assays in HEK293T cells with Mitf-luciferase reporter in the presence (+) or absence (−) of Pax3, Taz, Lats2, or Lats2KI.

(legend continued on next page)

in the analysis, which totaled 60 RFP+ cells in control embryos and 62 RFP+ cells in null embryos. Data are reported as an average percentage of each field totaled + SEM. Statistical differences between conditions were analyzed using a Student's t test.

Mouse Embryo Fibroblast Preparation

Mouse embryo fibroblasts (MEFs) were isolated from E14.5 $Taz^{flox/flox}$; $Yap^{flox/flox}$ embryos as described previously (Connor 2000). Briefly, E14.5 embryos were collected, the heads and internal organs were removed, and the remains were washed twice in PBS. Embryos were then dissociated by passage through a 16G needle and incubated in a trypsin solution for 5 min at 37°C. The resulting cells were then triturated and incubated for another 5 min at 37°C, and an equal volume of MEF media was added and incubated for 5 min at room temperature. After centrifugation, the cell pellet was resuspended in MEF media, plated, and incubated at 37°C. Cells were grown to confluence, then trypsinized and replated for treatment. In order to delete the floxed Taz and Yap65 alleles, MEFs were treated for 48 hr with an adeno-associated virus expressing a constitutively active Cre recombinase (AAV1-CMV-Cre, Penn Vector Core, University of Pennsylvania).

RNA Isolation, cDNA Synthesis, and Quantitative Real-Time PCR

RNA was harvested from a 1–100 mm dish of untreated or AAV1-CMV-Cre-treated $Taz^{flox/flox};Yap^{flox/flox}$ MEFs using the QIAGEN RNeasy kit following the manufacturer's instructions (QIAGEN). cDNA was synthesized with the Superscript III system (Invitrogen). Quantitative real-time PCR was performed in triplicate with SYBR green reagents (Applied Biosystems). Relative gene expression was normalized to *Gapdh.* Quantitative real-time PCR primer sequences are as follows:

Mitf forward: 5′-CGAGCTCATGGACTTTCCCTTA-3′
Mitf reverse: 5′-CTTGATGATCCGATTCACCAAA-3′
DCT forward: 5′-TTCGCAAAGGCTATGCGC-3′
DCT reverse: 5′-GTTACTACCCAGGTCAGGCCAG-3′
Taz forward: 5′-GAGAGGATTAGGATGCGTCAAG-3′
Taz reverse: 5′-GGATCTGAGCTACTGTTGGTG-3′
Yap forward: 5′-ACCATAAGAACAAGACCACATCC-3′
Yap reverse: 5′-CTTCACTGGAGCACTCTGAG-3′
Gapdh forward: 5′-CGTCCCGTAGACAAAATGGT-3′
Gapdh reverse: 5′-GAATTTGCCGTGAGTGGAGT-3′.

Mice

All mice were maintained on a mixed genetic background. *Wnt1-Cre* (Jiang et al., 2000), $Yap^{flox/+}$ (Xin et al., 2011), and $Taz^{flox/+}$ (Xin et al., 2013) alleles were genotyped as previously described. The $Yap^{flox/+}$ and $Taz^{flox/+}$ alleles were developed in the laboratory of Dr. Eric N. Olson at the University of Texas Southwestern Medical Center (Dallas, TX). *R26tdTomato* mice (B6.Cg-Gt(ROSA)26Sortm14(CAG-tdTomato)Hze/J) were obtained from Jackson Labs (strain number 007914). All animal protocols were approved by the University of Pennsylvania Institutional Animal Care and Use Committee.

SUPPLEMENTAL INFORMATION

Supplemental Information includes Supplemental Experimental Procedures, six figures, and one table and can be found with this article online at http://dx.doi.org/10.1016/j.celrep.2014.10.061.

AUTHOR CONTRIBUTIONS

L.J.M. designed and performed experiments, analyzed data, and wrote the paper. K.A.E. designed and performed experiments, analyzed data, and edited the manuscript. H.A. analyzed data. M.G., S.Y., and L.L. performed experiments. J.E.B. and J.B.H. helped with the experimental design of the high-throughput screen. E.N.O. provided the Yap and Taz floxed alleles. J.A.E. oversaw the entire project, designed experiments, analyzed data, and wrote the paper.

REFERENCES

Alarcón, C., Zaromytidou, A.I., Xi, Q., Gao, S., Yu, J., Fujisawa, S., Barlas, A., Miller, A.N., Manova-Todorova, K., Macias, M.J., et al. (2009). Nuclear CDKs drive Smad transcriptional activation and turnover in BMP and TGF-beta pathways. Cell *139*, 757–769.

Anbanandam, A., Albarado, D.C., Nguyen, C.T., Halder, G., Gao, X., and Veeraraghavan, S. (2006). Insights into transcription enhancer factor 1 (TEF-1) activity from the solution structure of the TEA domain. Proc. Natl. Acad. Sci. USA *103*, 17225–17230.

Bajard, L., Relaix, F., Lagha, M., Rocancourt, D., Daubas, P., and Buckingham, M.E. (2006). A novel genetic hierarchy functions during hypaxial myogenesis: Pax3 directly activates Myf5 in muscle progenitor cells in the limb. Genes Dev. *20*, 2450–2464.

Bondurand, N., Pingault, V., Goerich, D.E., Lemort, N., Sock, E., Le Caignec, C., Wegner, M., and Goossens, M. (2000). Interaction among SOX10, PAX3 and MITF, three genes altered in Waardenburg syndrome. Hum. Mol. Genet. *9*, 1907–1917.

Chi, N., and Epstein, J.A. (2002). Getting your Pax straight: Pax proteins in development and disease. Trends Genet. *18*, 41–47.

Connor, D.A. (2000). Mouse embryo fibroblast (MEF) feeder cell preparation. Curr. Protoc. Mol. Biol. *Chapter 23*, 23.2.1–23.2.7.

Degenhardt, K.R., Milewski, R.C., Padmanabhan, A., Miller, M., Singh, M.K., Lang, D., Engleka, K.A., Wu, M., Li, J., Zhou, D., et al. (2010). Distinct enhancers at the Pax3 locus can function redundantly to regulate neural tube and neural crest expressions. Dev. Biol. *339*, 519–527.

Di Palma, T., D'Andrea, B., Liguori, G.L., Liguoro, A., de Cristofaro, T., Del Prete, D., Pappalardo, A., Mascia, A., and Zannini, M. (2009). TAZ is a coactivator for Pax8 and TTF-1, two transcription factors involved in thyroid differentiation. Exp. Cell Res. *315*, 162–175.

Diao, Y., Guo, X., Li, Y., Sun, K., Lu, L., Jiang, L., Fu, X., Zhu, H., Sun, H., Wang, H., and Wu, Z. (2012). Pax3/7BP is a Pax7- and Pax3-binding protein that regulates the proliferation of muscle precursor cells by an epigenetic mechanism. Cell Stem Cell *11*, 231–241.

(I) Results of dual luciferase reporter assays in HEK293T cells with Mitf-luciferase reporter in the presence (+) or absence (−) of Pax3, Yap65, Lats2, or Lats2KI. In all experiments, luciferase activity was first normalized to the activity of a cotransfected renilla luciferase construct, then to the activity observed in the absence of specified cDNAs (lane 1). All experiments were performed in duplicate on a minimum of three individual occasions. Data depicted are the mean + SEM. Statistics were completed using an ANOVA with a Tukey-Kramer post hoc comparison test. ***p < 0.001, **p < 0.01, *p < 0.05

Dong, J., Feldmann, G., Huang, J., Wu, S., Zhang, N., Comerford, S.A., Gayyed, M.F., Anders, R.A., Maitra, A., and Pan, D. (2007). Elucidation of a universal size-control mechanism in Drosophila and mammals. Cell *130*, 1120–1133.

Dupont, S., Morsut, L., Aragona, M., Enzo, E., Giulitti, S., Cordenonsi, M., Zanconato, F., Le Digabel, J., Forcato, M., Bicciato, S., et al. (2011). Role of YAP/TAZ in mechanotransduction. Nature *474*, 179–183.

Epstein, J., Cai, J., Glaser, T., Jepeal, L., and Maas, R. (1994). Identification of a Pax paired domain recognition sequence and evidence for DNA-dependent conformational changes. J. Biol. Chem. *269*, 8355–8361.

Epstein, J.A., Lam, P., Jepeal, L., Maas, R.L., and Shapiro, D.N. (1995). Pax3 inhibits myogenic differentiation of cultured myoblast cells. J. Biol. Chem. *270*, 11719–11722.

Ferrigno, O., Lallemand, F., Verrecchia, F., L'Hoste, S., Camonis, J., Atfi, A., and Mauviel, A. (2002). Yes-associated protein (YAP65) interacts with Smad7 and potentiates its inhibitory activity against TGF-beta/Smad signaling. Oncogene *21*, 4879–4884.

Gee, S.T., Milgram, S.L., Kramer, K.L., Conlon, F.L., and Moody, S.A. (2011). Yes-associated protein 65 (YAP) expands neural progenitors and regulates Pax3 expression in the neural plate border zone. PLoS ONE *6*, e20309.

Goulding, M.D., Chalepakis, G., Deutsch, U., Erselius, J.R., and Gruss, P. (1991). Pax-3, a novel murine DNA binding protein expressed during early neurogenesis. EMBO J. *10*, 1135–1147.

Harvey, K.F., Pfleger, C.M., and Hariharan, I.K. (2003). The Drosophila Mst ortholog, hippo, restricts growth and cell proliferation and promotes apoptosis. Cell *114*, 457–467.

Jiang, X., Rowitch, D.H., Soriano, P., McMahon, A.P., and Sucov, H.M. (2000). Fate of the mammalian cardiac neural crest. Development *127*, 1607–1616.

Justice, R.W., Zilian, O., Woods, D.F., Noll, M., and Bryant, P.J. (1995). The Drosophila tumor suppressor gene warts encodes a homolog of human myotonic dystrophy kinase and is required for the control of cell shape and proliferation. Genes Dev. *9*, 534–546.

Kanai, F., Marignani, P.A., Sarbassova, D., Yagi, R., Hall, R.A., Donowitz, M., Hisaminato, A., Fujiwara, T., Ito, Y., Cantley, L.C., and Yaffe, M.B. (2000). TAZ: a novel transcriptional co-activator regulated by interactions with 14-3-3 and PDZ domain proteins. EMBO J. *19*, 6778–6791.

Kim, E.A., Noh, Y.T., Ryu, M.J., Kim, H.T., Lee, S.E., Kim, C.H., Lee, C., Kim, Y.H., and Choi, C.Y. (2006). Phosphorylation and transactivation of Pax6 by homeodomain-interacting protein kinase 2. J. Biol. Chem. *281*, 7489–7497.

Komuro, A., Nagai, M., Navin, N.E., and Sudol, M. (2003). WW domain-containing protein YAP associates with ErbB-4 and acts as a co-transcriptional activator for the carboxyl-terminal fragment of ErbB-4 that translocates to the nucleus. J. Biol. Chem. *278*, 33334–33341.

Lang, D., Chen, F., Milewski, R., Li, J., Lu, M.M., and Epstein, J.A. (2000). Pax3 is required for enteric ganglia formation and functions with Sox10 to modulate expression of c-ret. J. Clin. Invest. *106*, 963–971.

Lang, D., Lu, M.M., Huang, L., Engleka, K.A., Zhang, M., Chu, E.Y., Lipner, S., Skoultchi, A., Millar, S.E., and Epstein, J.A. (2005). Pax3 functions at a nodal point in melanocyte stem cell differentiation. Nature *433*, 884–887.

Lei, Q.Y., Zhang, H., Zhao, B., Zha, Z.Y., Bai, F., Pei, X.H., Zhao, S., Xiong, Y., and Guan, K.L. (2008). TAZ promotes cell proliferation and epithelial-mesenchymal transition and is inhibited by the hippo pathway. Mol. Cell. Biol. *28*, 2426–2436.

Lin, Y., Khokhlatchev, A., Figeys, D., and Avruch, J. (2002). Death-associated protein 4 binds MST1 and augments MST1-induced apoptosis. J. Biol. Chem. *277*, 47991–48001.

Mansouri, A., and Gruss, P. (1998). Pax3 and Pax7 are expressed in commissural neurons and restrict ventral neuronal identity in the spinal cord. Mech. Dev. *78*, 171–178.

Milewski, R.C., Chi, N.C., Li, J., Brown, C., Lu, M.M., and Epstein, J.A. (2004). Identification of minimal enhancer elements sufficient for Pax3 expression in neural crest and implication of Tead2 as a regulator of Pax3. Development *131*, 829–837.

Morin-Kensicki, E.M., Boone, B.N., Howell, M., Stonebraker, J.R., Teed, J., Alb, J.G., Magnuson, T.R., O'Neal, W., and Milgram, S.L. (2006). Defects in yolk sac vasculogenesis, chorioallantoic fusion, and embryonic axis elongation in mice with targeted disruption of Yap65. Mol. Cell. Biol. *26*, 77–87.

Murakami, M., Nakagawa, M., Olson, E.N., and Nakagawa, O. (2005). A WW domain protein TAZ is a critical coactivator for TBX5, a transcription factor implicated in Holt-Oram syndrome. Proc. Natl. Acad. Sci. USA *102*, 18034–18039.

Murakami, M., Tominaga, J., Makita, R., Uchijima, Y., Kurihara, Y., Nakagawa, O., Asano, T., and Kurihara, H. (2006). Transcriptional activity of Pax3 is co-activated by TAZ. Biochem. Biophys. Res. Commun. *339*, 533–539.

Potterf, S.B., Furumura, M., Dunn, K.J., Arnheiter, H., and Pavan, W.J. (2000). Transcription factor hierarchy in Waardenburg syndrome: regulation of MITF expression by SOX10 and PAX3. Hum. Genet. *107*, 1–6.

Relaix, F., Polimeni, M., Rocancourt, D., Ponzetto, C., Schäfer, B.W., and Buckingham, M. (2003). The transcriptional activator PAX3-FKHR rescues the defects of Pax3 mutant mice but induces a myogenic gain-of-function phenotype with ligand-independent activation of Met signaling in vivo. Genes Dev. *17*, 2950–2965.

Soleimani, V.D., Punch, V.G., Kawabe, Y., Jones, A.E., Palidwor, G.A., Porter, C.J., Cross, J.W., Carvajal, J.J., Kockx, C.E., van IJcken, W.F., et al. (2012). Transcriptional dominance of Pax7 in adult myogenesis is due to high-affinity recognition of homeodomain motifs. Dev. Cell *22*, 1208–1220.

Strano, S., Munarriz, E., Rossi, M., Castagnoli, L., Shaul, Y., Sacchi, A., Oren, M., Sudol, M., Cesareni, G., and Blandino, G. (2001). Physical interaction with Yes-associated protein enhances p73 transcriptional activity. J. Biol. Chem. *276*, 15164–15173.

Tapon, N., Harvey, K.F., Bell, D.W., Wahrer, D.C., Schiripo, T.A., Haber, D., and Hariharan, I.K. (2002). salvador Promotes both cell cycle exit and apoptosis in Drosophila and is mutated in human cancer cell lines. Cell *110*, 467–478.

Varelas, X., Sakuma, R., Samavarchi-Tehrani, P., Peerani, R., Rao, B.M., Dembowy, J., Yaffe, M.B., Zandstra, P.W., and Wrana, J.L. (2008). TAZ controls Smad nucleocytoplasmic shuttling and regulates human embryonic stem-cell self-renewal. Nat. Cell Biol. *10*, 837–848.

Watanabe, A., Takeda, K., Ploplis, B., and Tachibana, M. (1998). Epistatic relationship between Waardenburg syndrome genes MITF and PAX3. Nat. Genet. *18*, 283–286.

Wu, S., Huang, J., Dong, J., and Pan, D. (2003). hippo encodes a Ste-20 family protein kinase that restricts cell proliferation and promotes apoptosis in conjunction with salvador and warts. Cell *114*, 445–456.

Xin, M., Kim, Y., Sutherland, L.B., Qi, X., McAnally, J., Schwartz, R.J., Richardson, J.A., Bassel-Duby, R., and Olson, E.N. (2011). Regulation of insulin-like growth factor signaling by Yap governs cardiomyocyte proliferation and embryonic heart size. Sci. Signal. *4*, ra70.

Xin, M., Kim, Y., Sutherland, L.B., Murakami, M., Qi, X., McAnally, J., Porrello, E.R., Mahmoud, A.I., Tan, W., Shelton, J.M., et al. (2013). Hippo pathway effector Yap promotes cardiac regeneration. Proc. Natl. Acad. Sci. USA *110*, 13839–13844.

Xu, T., Wang, W., Zhang, S., Stewart, R.A., and Yu, W. (1995). Identifying tumor suppressors in genetic mosaics: the Drosophila lats gene encodes a putative protein kinase. Development *121*, 1053–1063.

Zaidi, S.K., Sullivan, A.J., Medina, R., Ito, Y., van Wijnen, A.J., Stein, J.L., Lian, J.B., and Stein, G.S. (2004). Tyrosine phosphorylation controls Runx2-mediated subnuclear targeting of YAP to repress transcription. EMBO J. *23*, 790–799.

Zhang, H., Liu, C.Y., Zha, Z.Y., Zhao, B., Yao, J., Zhao, S., Xiong, Y., Lei, Q.Y., and Guan, K.L. (2009). TEAD transcription factors mediate the function of TAZ in cell growth and epithelial-mesenchymal transition. J. Biol. Chem. *284*, 13355–13362.

Zhao, B., Ye, X., Yu, J., Li, L., Li, W., Li, S., Yu, J., Lin, J.D., Wang, C.Y., Chinnaiyan, A.M., et al. (2008). TEAD mediates YAP-dependent gene induction and growth control. Genes Dev. *22*, 1962–1971.